World Journal of Advanced Research and Reviews
eISSN: 2581-9615 CODEN (USA): WJARAI
Cross Ref DOI: 10.30574/wjarr
Journal homepage: https://wjarr.com/

(RESEARCH ARTICLE)

Check for updates

Forecasting monthly rainfall using autoregressive integrated moving average model (ARIMA): A case study of Fada N'Gourma station in Burkina Faso

Bontogho Tog-Noma Patricia Emma [1,*], Maré Boussa Tockville [2], Yangouliba Gnibga Issoufou [3] and Gaba Olayemi Ursula Charlène [4]

[1] *High Institute of Sustainable Development, University of Fada N'Gourma, Burkina Faso.*
[2] *University Joseph Ki Zerbo, SVT, Burkina Faso.*
[3] *Doctoral Reasearch Program in Climate Change and water Resources Universty of Abomey Calavy, Benin.*
[4] *National Institue of Water, University of Abomey-Calavi/Benin.*

World Journal of Advanced Research and Reviews, 2023, 20(03), 251–262

Publication history: Received on 17 October 2023; revised on 28 November 2023; accepted on 01 December 2023

Article DOI: https://doi.org/10.30574/wjarr.2023.20.3.2442

Abstract

Climate related hazards are challenging vulnerable communities and decision makers at any mitigation and adaptation planning stage. Accurate knowledge on projected climate variables such as rainfall is crucial in setting efficient adaptation strategies. The present study seeks to determine an optimum model to predict rainfall patterns within Fada N'Gourma. To this end, the autoregressive integrated moving average model (ARIMA) were fit to the monthly rainfall record for Fada N'Gourma meteorological stations spanning from 1981 to 2021. Then, the Box-Jenkins method has been applied under R programming language to identify the appropriate ARIMA $(p, d, q) * (P, D, Q)$ model that fits the rainfall records. The stationarity of the dataset has been checked based on Augmented Dicky fuller test. The best model used to predict the next ten-year rainfall was selected based on Akaike information criterion (AIC) and Bayesian information criterion (BIC). The efficiency of the model was evaluated by the root mean square errors (RMSE) and the mean squared error (MSE). The results demonstrate that the ARIMA model (5,0,0)(2,1,0)[12] is an appropriate forecasting tool to predict the monthly rainfall across Fada N'Gourma. Base on this model, rainfall forecast for 10 years was then achieved. The Mann-Kendall trend test for the projected rainfall shows a z = 0.89 and a value of Sen's slope up to 0.88 depicting an increasing trend of the annual rainfall within Fada Gourma by 2030.

Keywords: Rainfall forecast; ARIMA model; Fada N'Gourma; AIC; BIC.

1. Introduction

Hydrological processes are highly dependent on rainfall [1, 2]. Indeed, Cristiano et al. [3] rightly emphasized that hydrological processes are characterized by high variability in space and time concordantly to rainfall changes. Additionally, Van Loon et al. [4] stated that a deficit in rainfall strongly influences the hydrological regimes of streamflow worldwide. Addressing historical, current and future rainfall features remains a tremendous endeavor for water resources managers. Niemczynowicz et al. [5] reported that sufficient information related to the spatial distribution of short-term rainfall is required to reduce the uncertainties in urban runoff estimation. In Burkina Faso, nearly 80% of population is involved in agriculture. However, over the last few decades, the country's food security and economic developments are exacerbated by climate change and its variability as reported by influential papers [6, 7]. Many studies have dealt with rainfall modeling in Burkina Faso [8, 9, 10]. A few of them is discussed briefly. Ibrahim et al. [11] applied a linear regression model to forecast rainfall data for 2021 to 2050. They found high uncertainties in the projected change in annual rainfall for West Africa. Messager et al. [12] used the hydrologic model (ABC) to model observed and simulated rainfall over the Sirba watershed. The overall result has revealed that the representation of daily rainfall was

* Corresponding author: Bontogho Tog-Noma Patricia Emma.

not sufficiently accurate to simulate the hydrologic response of the watershed. Geetha et al. [13] stated that forecasting is a complex phenomenon bounded of uncertainties and characterized by the ability to determine a system features in the future. According to Petropoulos et al. [14], forecasting has always been at the cutting edge of decision making and planning. Indeed, in water related sectors for instance, rainfall forecasting provides relevant insights for decisions making [15,16,17,18]. Therefore, rainfall forecasting is crucial for mitigation and adaptation strategies both in flash flood regions and in drought proned areas since it helps to design anticipated plans that could be implemented to avoid lives and economic losses. In addition, rainfall forecasting is essential for efficient water resource planning and management [19, 20, 21]. However, weather forecasting is still challenging researchers [22, 23, 24].There are several methods pertaining to time series forecasting. French et al. [25] applied a neural network to forecast rainfall intensity fields in space and time. Fahad et al. [26] applied a deep forecasting model based on optimized Gated Recurrent Unit (GRU) neural network to predict rainfall in Pakistan based on the 30 years of climate data from 1991 to 2020. Hossain et al. [27] applied a linear multiple regression (MR) models to forecast rainfall in Australia. In Burkina Faso, a large body of literature has been concerned with rainfall forecasting [28, 29, 30, and 31]. The main purpose of this work is to identify the optimum model for predicting Fada N'Gourma rainfall. For this purpose, the , Autoregressive Integrated Moving Average (ARIMA) method has been applied to monthly rainfall data covering the period 1981-2021 in order to forecast rainfall in Fada N'Gourma.

2. Materials and Methods

2.1. Presentation of the study Area and Rainfall Data

The present study was conducted in Fada N'Gourma located in eastern Burkina Faso. Geographically, Fada N'Gourma is bounded by latitude 12° 4′ 0″ Nord and longitude 0° 21′ 0″ East with an elevation of 309m. Fada N'Gourma is in the Soudano Sahelian zone characterized by a short rainy season spanning from May to September with a peak generally in August and a long dry season spanning from October to April. Fada N'Gourma is characterized by an annual mean temperature of 28.9°C, an annual mean relative humidity of 50.4%. The major soils groups present within Fada N'Gourma are tropical ferruginous soils, unsuitable for agriculture, hydromorphic pseudo-gley soils and poorly evolved pseudo-gley alluvial soils [32]. The vegetation is dominated by tree and shrub savana. The 2019 census of the population had recorded 437,310 inhabitants within the study area of which women represent the largest proportion with a rate of 51.8% compared to 48.2% of men [33]. A monthly rainfall record from 1981 to 2021 is applied in the framework of this study.

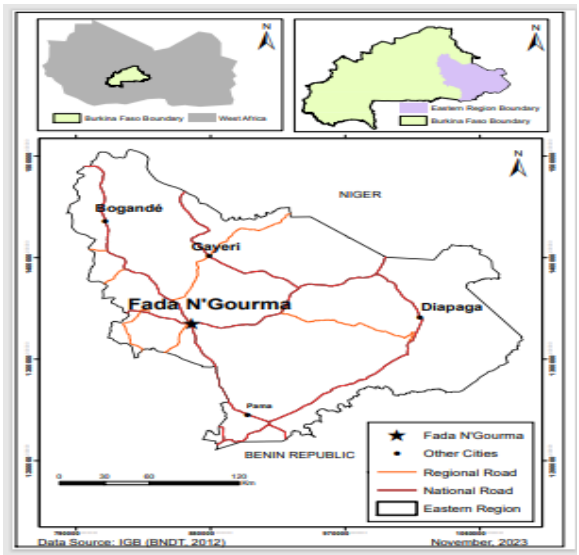

Figure 1 Study Area

2.2. ARIMA model

Box and Jenkins [34] suggested the ARIMA model for time series analysis and prediction based on the conversion of a non-stationary time series into a stationary time series. The main advantage of this model is its ability to detect seasonal changes and consider serial correlation within the time series [35]. The model has three components, which are the autoregressive component (AR), the moving average component (MA), and the combination of both parts integrated in

the model by the differencing order. Filder et al. [36] stated that applying ARIMA models on any time series show patterns with no random white noise and non-seasonal. In addition, Ariyo et al. [37] highlighted that ARIMA models generate short-term forecasts with efficient capability outperformed complex structural models. In the ARIMA (*p, d, q*) model, *p* represents the autoregressive term, *d* refers to the trend term, and *q* stands for the moving average term.

2.3. Autoregressive (AR) model

In the ARIMA model, the acronym 'AR (*p*)' in ARIMA model stands for the Autoregressive model of order (*p*). 'AR' is represented by the following formula:

$$x_t = \sum_{j=1}^{p} \emptyset_j x_{t-1} + \varepsilon_t$$

Where:

x represents the observation at time t,
$\emptyset_j$ stands for the j^{th} autoregressive parameter.
ε_t is the independent random variable representing the error term at time t
x_{t-1} stands for the time series at the time *(t-1)*, *p* = order of autoregressive process.

2.4. Moving-average (MA) model

In the ARIMA model, MA (*q*) is identified as a moving average model of the order q and is given by:

$$x_t = \varepsilon_t - \sum_{j=0}^{q} \theta_j \varepsilon_{t-1}$$

Where: θ_j is the j^{th} moving average parameter

q is the order of the moving average process

The following equation shows the expression of the future value of any variable in ARIMA model which is a combination of linear to the past values and errors:

$$Yt = \phi 0 + \phi 1 Yt - 1 + \phi 2 Yt - 2 + \ldots + \phi p Yt - p + \varepsilon t - \theta 1 \varepsilon t - 2 - \ldots - \theta q \varepsilon t - q$$

Yt stands for the actual value,
εt refers to the random error at *t*,
ϕi and θj represent the coefficients,
p and *q* are integers that are often referring respectively to autoregressive and moving average.

ARIMA method was adopted in this study which involved model identification, parameter estimation and diagnostic checking (residual analysis), and the forecasting.

2.5. Model Identification

ARIMA model requires stationary time series. Thus, checking the stationarity of the data is the first step in ARIMA forecasting. To achieve this, an estimation of the orders (*p, d,* and *q*) for the autoregressive and the moving average components of the model is required. A time series is stated stationary when the values of a parameter fluctuates around a constant mean and variance independently of time. During the process of model identification, the non-stationary data are converted to a stationary series through a differencing procedure that allow to identify the accurate value of *d*.

2.6. Model Estimation

Model estimation is an important step in ARIMA modeling. During this process, the technique of maximum likelihood estimation (MLE) is applied to attempt to identify the accurate model for the forecasting. The principle of maximum likelihood parameter estimation is to find the parameter values that make the observed data most likely [38, 39, 40].

2.7. Model Checking

The aim of the model checking is to check the model for adequacy. The Ljung-Box Q statistic provides an overall check of the model adequacy. Indeed, the Ljung–Box test is a type of typical statistical test of whether any autocorrelation of a time series is different from zero. The Ljung–Box Q statistic is given as:

$$Q_m = n(n+2)\sum_{k=1}^{m}\frac{r_k^2(e)}{n-k} \sim X_{m-r}^2$$

Where: $r_k(e)$ stands for the residual autocorrelation at lag k;

n is the number of residuals;

m indicates the number of time lags included in the test;

In addition to the Ljung-Box Q statistics, a multi-criterion performance evaluation was applied using Augmented Dickey-Fuller (ADF) test, Root Mean Square Error (RMSE) and Mean Absolute Error (MAE).

The RMSE and MAE are given by:

$$RMSE = \sqrt{\frac{\sum_{k=1}^{N}(t(k)-a(k)^2)}{N}} \qquad MAE = \frac{1}{N}\sum_{k=1}^{N}|t(k)-a(k)|$$

The forecasting was further extended by estimating the Mann–Kendall parameter and the Sen's Slope value. The Mann–Kendall and the Sen's Slope estimator tests are both widely used in determining trend and magnitude in time series [41,42, 43]. Mann-Kendall is a non-parametric trend test expressed as follows:

$$\mathbf{Zs} = \begin{cases} \dfrac{\boldsymbol{S-1}}{\sqrt{\boldsymbol{Var(S)}}}, & \boldsymbol{S>0} \\ \mathbf{0}, & \mathbf{S=0} \\ \dfrac{\boldsymbol{S+1}}{\sqrt{\boldsymbol{Var(S)}}}, & \boldsymbol{S<0} \end{cases}$$

A positive Zs value indicates an upwarding trend while a negative Zs shows a downwarding trend.

The Sen'slope non-parametric test is estimated based on the following the equations:

$$\boldsymbol{\beta i} = \mathbf{Median}\left[\frac{\mathbf{x_j - x_k}}{\mathbf{j-k}}\right] \quad \forall\ (k < j)$$

Where:

$\mathbf{X_j}$ and $\mathbf{X_k}$ correspond to the values data at time j and k, respectively, and time j stands for the value data after time k (k ≤ j). Therefore, the median of "n" values of **βi** refers to the Sen's slope estimator test where negative **βi** value highlighting a downwarding trend while positive **βi** value shows a rising trend.

3. Results and Discussion

3.1. Data analysis

The figure 2 provides the decomposition of Fada N'Gourma monthly rainfall time series. As stated by [44] a time series decomposition is widely used in many fields including economics, finance, managing production operations, analysis of

political and social policy sessions. According to Bandara et al. [45] time series decomposition facilitates forecasting. A time series decomposition is expressed by:

$Yt = Tt + St + Rt$

Where Tt represents the trend component, St Stands for the seasonal component, and Rt refers to the random component or noise.

The plot shows considerable variation in rainfall amount over the years. This time series displays a very cyclical component of the rainfall within the study area.

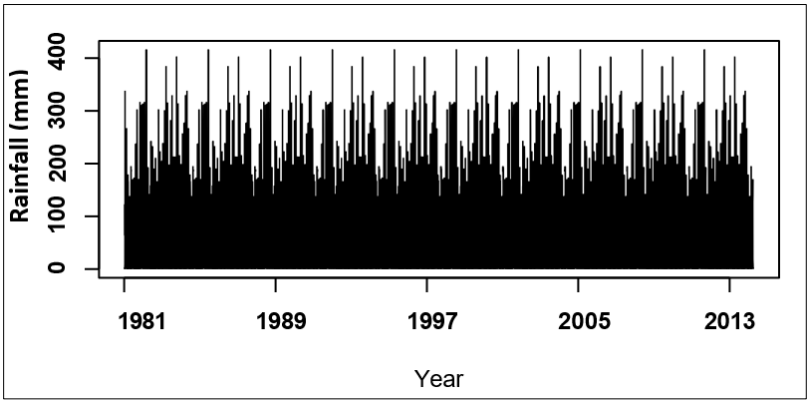

Figure 2 Time series plot of Fada N'Gourma monthly rainfall

Figure 3 illustrates the decomposition of the time series data into four components (trend, seasonality, random and observed). This decomposition shows that the time series has a seasonal pattern with high a variability across years. A slight increase in observed during the last decade. The rainfall has a unimodal trend characterized by a dry season lasting from January to May and a rainy season lasting from June to September.

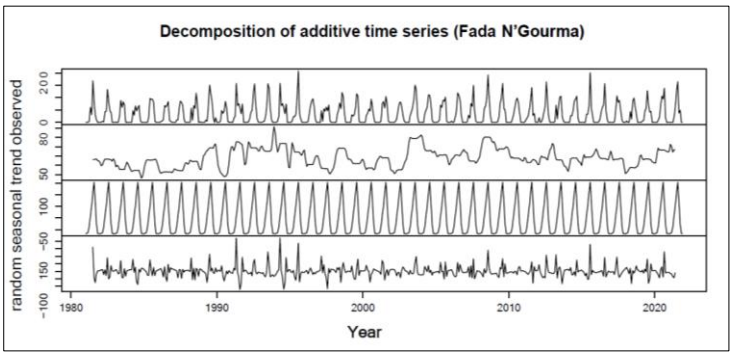

Figure 3 Illustration of additive time series decomposition for monthly rainfall at Fada N'Gourma station

Figure 4 provides the adjusted monthly rainfall plot at Fada N'Gourma station. The result shows that rainfall has a seasonality pattern without any trends occurring; the higher value of rainfall is reached in August and the dry season lies from September to May. This pattern has been always repeated yearly from 1983 to 2021.

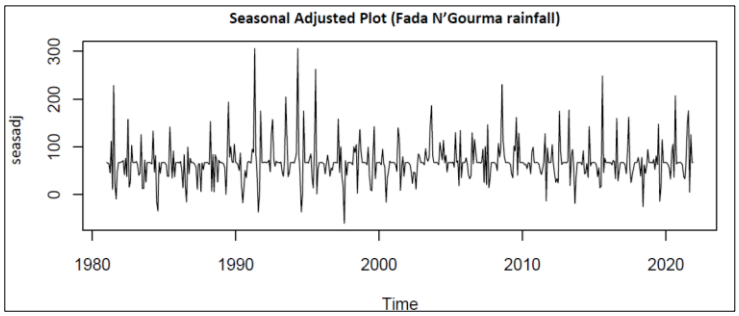

Figure 4 Illustration of adjusted monthly rainfall at Fada N'Gourma station

The Figure 5-a) presents the correlogram of the auto-correlation function (ACF) for lags 1 to 20 of the first order differenced time series of the rainfall patterns within the study area. ACF is defined as a graph showing the correlation between the points in a dataset. In ACF, the correlation coefficient is in the y-axis whereas the number of lags is shown in the x-axis. The ACF plot of the monthly rainfall in Fada N'Gourma shows a positive correlation at lag 1, 2 and at lag 10 until lag 14. On another note, negative correlation is found for lag 3 to 9 and lag15 to 20. The Figure 5-b) represents the plot of Partial Auto-Correlation Function (Pacf) for lags 1 to 20 of the first order differenced time series of Fada N'Gourma meteorological station rainfall records. Partial autocorrelation refers to a summary of the relationship between observations in a dataset with observations at prior time steps with the relationships of intervening observations removed. In Pacf, the correlation coefficient is in the y-axis whereas the number of lags is shown in the x-axis. The Pacf plot of the monthly rainfall in Fada N'Gourma shows a positive correlation at lag 1 and 11 until lag 15. Futhermore, negative correlation is found for lag 2 to 9 and lag16 to 20. Both ACF and Pacf are confirming the seasonal behavior of the time serie analysed.

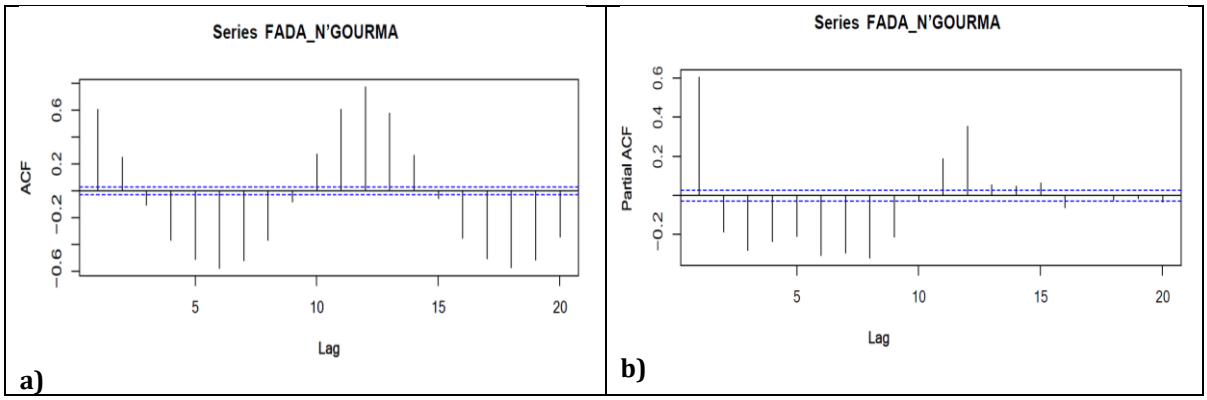

Figure 5a) Autocorrelation function plot of Monthly Rainfall in Fada N'Gourma. Figure 6b): Partial Autocorrelation function plot of Monthly Rainfall in Fada N'Gourma

The coefficients of the autocorrelation function and the partial autocorrelation for the twenty lags are provided in table 1. A positive correlation indicates that large current values correspond with large values at the specified lag while a negative correlation indicates that large current values correspond with small values at the specified lag. However, the absolute value of a correlation is a measure of the strength of the association, with larger absolute values indicating stronger relationships. Strong correlations (> 0.6) are detected for lag 1, 11 and 12 as far as ACF is concerned while in Pacf the strong correlation is only detected at lag 1.

Table 1 ACF and PACF coefficients by lags for the monthly rainfall in Fada N'Gourma

Lag	ACF	PACF	Lag	ACF	PACF
1	0.606	0.606	11	0.604	0.188
2	0.249	-0.186	12	0.774	0.354
3	-0.107	-0.282	13	0.577	0.053
4	-0.370	-0.235	14	0.264	0.049

5	-0.510	-0.211	15	-0.061	0.063
6	-0.577	-0.309	16	-0.356	-0.062
7	-0.521	-0.293	17	-0.506	0.000
8	-0.368	-0.320	18	-0.573	-0.023
9	-0.085	-0.214	19	-0.514	-0.016
10	0.275	-0.031	20	-0.347	-0.033

3.2. Test for stationarity: Augmented Dickey-Fuller Test

Dickey–Fuller test has been suggested by [46] in order to examine the null hypothesis of ARIMA against stationary and alternatively. ADF test is the extended version of Dickey Fuller test and is commonly used to test the unit root. The ADF statistic, used in the test, is a negative number. The more negative it is, the stronger the rejection of the hypothesis that there is a unit root at some level of confidence. The ADF test result, as obtained upon application, shows a Dickey-Fuller value of -15.592 at lag order = 17 and a p-value of 0.01 and confirms the stationarity in the data.

3.3. Correlogram and Partial Correlogram of residuals

The figure 6 below displays the correlogram of the auto-correlation function (ACF) and Partial auto-correlation function (Pacf) resulting from the residuals. The ACF plot of residual shows a positive correlation at lag 9, 10, 11, 15 and lag 17 to lag 20. Negative correlation is detected for lag 3 to 8 and lag 12, 13 and 16. The Pacf plot of the residuals shows a positive correlation at lag 9, 10, 11, 14 ,15, 17, 18 and 20 while negative correlation are depicted in lag 4, 5, 6, 8 ,12, 13, 16 and 19. Therefore both ACF and Pacf for residuals are confirming the seasonality of the time series.

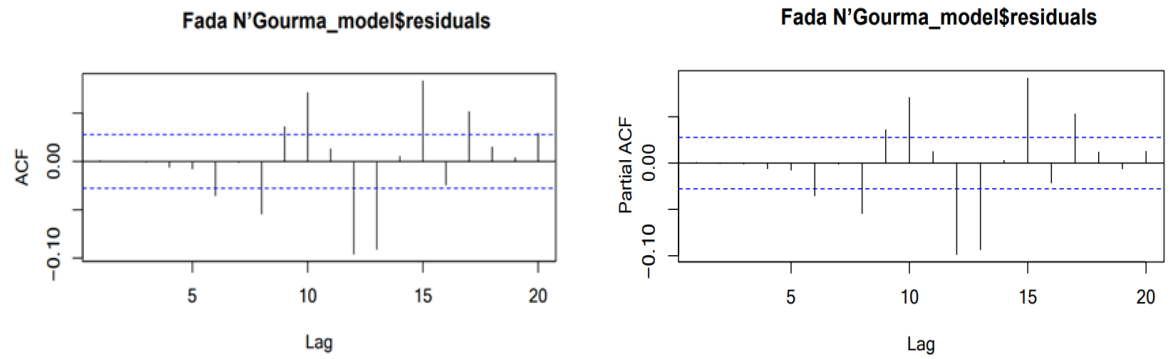

A B

Figure 6 a) Plot of Acf's residuals from ARIMA (5,0,0)(2,1,0)[12] model; b) Plot of the Pacf' residuals from ARIMA (5,0,0)(2,1,0)[12] model.

The table below shows the values of the correlation resulting from the residuals. The absolute value of the correlation for each stage is almost zero (0) depicting a weak association among the variables. Indeed, no significant correlation can be identified. The correlation within the time series is therefore remove and the data can be applied for the forecasting as required in ARIMA modeling.

Table 2 Residuals ACF and PACF coefficients by lags for the monthly rainfall in Fada N'Gourma

Lag	ACF	PACF	Lag	ACF	PACF
1	0.001	0.001	11	0.013	0.013
2	-0.001	-0.001	12	-0.096	-0.099
3	-0.001	-0.001	13	-0.091	-0.094
4	-0.006	-0.006	14	0.006	0.003

5	-0.008	-0.008	15	0.084	0.092
6	-0.036	-0.036	16	-0.025	-0.022
7	-0.002	-0.001	17	0.052	0.053
8	-0.055	-0.055	18	0.015	0.012
9	0.036	0.036	19	0.004	-0.006
10	0.072	0.071	20	0.030	0.013

Table 3. presents the The ARIMA model (5,0,0)(2,1,0)[12] was selected as the appropriate model after assessing its performance and analyzing its residuals.

Table 3 Fitting models using approximation

Fitting models using approximations					
ARIMA(2,0,2)(1,1,1)[12]	WD	Inf	ARIMA(3,0,1)(2,1,1)[12]	WD	Inf
ARIMA(0,0,0)(0,1,0)[12]	WD	54377.93	ARIMA(3,0,1)(1,1,1)[12]	WD	Inf
ARIMA(1,0,0)(1,1,0)[12]	WD	53241.3	ARIMA(3,0,0)(2,1,0)[12]	WD	52050.21
ARIMA(0,0,1)(0,1,1)[12]	WD	Inf	ARIMA(4,0,1)(2,1,0)[12]	WD	52025.36
ARIMA(0,0,0)(0,1,0)[12]		54375.93	ARIMA(4,0,1)(1,1,0)[12]	WD	53133.52
ARIMA(1,0,0)(0,1,0)[12]	WD	54360.64	ARIMA(4,0,1)(2,1,1)[12]	WD	Inf
ARIMA(1,0,0)(2,1,0)[12]	WD	52094.06	ARIMA(4,0,1)(1,1,1)[12]	WD	Inf
ARIMA(1,0,0)(2,1,1)[12]	WD	Inf	ARIMA(4,0,0)(2,1,0)[12]	WD	52045.31
ARIMA(1,0,0)(1,1,1)[12]	WD	Inf	ARIMA(5,0,1)(2,1,0)[12]	WD	51999.64
ARIMA(0,0,0)(2,1,0)[12]	WD	52092.72	ARIMA(5,0,1)(1,1,0)[12]	WD	53036.78
ARIMA(0,0,0)(1,1,0)[12]	WD	53247.92	ARIMA(5,0,1)(2,1,1)[12]	WD	Inf
ARIMA(0,0,0)(2,1,1)[12]	WD	Inf	ARIMA(5,0,1)(1,1,1)[12]	WD	Inf
ARIMA(0,0,0)(1,1,1)[12]	WD	Inf	ARIMA(5,0,0)(2,1,0)[12]	WD	52043.11
ARIMA(0,0,1)(2,1,0)[12]	WD	52092.81	ARIMA(5,0,2)(2,1,0)[12]	WD	Inf
ARIMA(1,0,1)(2,1,0)[12]	WD	53237.15	ARIMA(4,0,2)(2,1,0)[12]	WD	52025.28
ARIMA(1,0,1)(1,1,0)[12	WD	53237.15	ARIMA(5,0,1)(2,1,0)[12]		51997.84
ARIMA(1,0,1)(2,1,1)[12]	WD	Inf	ARIMA(5,0,1)(1,1,0)[12]		53034.96
ARIMA(1,0,1)(1,1,1)[12]	WD	Inf	ARIMA(5,0,1)(2,1,1)[12]		Inf
ARIMA(2,0,1)(2,1,0)[12]	WD	52053.81	ARIMA(5,0,1)(1,1,1)[12]		Inf
ARIMA(2,0,1)(1,1,0)[12]	WD	Inf	ARIMA(4,0,1)(2,1,0)[12]		52023.36
ARIMA(2,0,1)(2,1,1)[12]	WD	Inf	ARIMA(5,0,0)(2,1,0)[12]		52041.11
ARIMA(2,0,1)(1,1,1)[12]	WD	Inf	ARIMA(5,0,2)(2,1,0)[12]		Inf
ARIMA(2,0,0)(2,1,0)[12]	WD	52078.94	ARIMA(4,0,0)(2,1,0)[12]		52043.32
ARIMA(3,0,1)(2,1,0)[12]	WD	52049.76	ARIMA(4,0,2)(2,1,0)[12]		52023.37
ARIMA(3,0,1)(1,1,0)[12]	WD	Inf			

The re-fitting model without approximations provided in table 2 shows that ARIMA (5,0,0)(2,1,0) with non-zero mean of 52145.24 is the best model for rainfall prediction within Fada N'Gourma.

Table 4 Re-fitting models without approximations

Re-fitting the best model(s) without approximations		
ARIMA(5,0,1)(2,1,0)[12]		Inf
ARIMA(5,0,1)(2,1,0)[12	with drift	Inf
ARIMA(4,0,1)(2,1,0)[12		Inf
ARIMA(4,0,2)(2,1,0)[12]		Inf
ARIMA(4,0,2)(2,1,0)[12]	with drift	Inf
ARIMA(4,0,1)(2,1,0)[12	with drift	Inf
ARIMA(5,0,0)(2,1,0)[12		52145.24

The maximum likelihood estimates of the ARIMA (5,0,0)(2,1,0)[12] model and their standard errors are presented in Table 5. The Ljung–Box test is a type of typical statistical test of whether any autocorrelation of a time series is different from zero. The Ljung–Box test at lag 8 for Fada rainfall station shows $x^2 = 21.803$, df = 8 and p-value = 0.005294.

Table 5 Maximum likelihood estimates of the ARIMA (5,0,0)(2,1,0)[12] model and their standard errors

Coefficients	**ar1**	**ar2**	**ar3**	**ar4**	**ar5**	**sar1**	**sar2**
Estimate	-0.0261	-0.0618	-0.0775	-0.0280	0.0305	-0.6514	-0.4475
Standard Error	0.0143	0.0142	0.0142	0.0143	0.0142	0.0129	0.0129

3.4. Performance evaluation criteria and trend assessment

Table 6 provides information of the goodness-of-fit statistics for the ARIMA(5,0,0)(2,1,0)[12] model. The statistical indicators ME= -0.05, RMSE = 45.23, MAE = 28.02, MASE = 0.86 and ACF1= 0.001. The study revealed that ARIMA(5,0,0)(2,1,0)[12] model can be used as an appropriate forecasting tool to predict the monthly rainfall in Fada N'Gourma.

Table 6 Value of performance evaluation criteria

	ME	**RMSE**	**MAE**	**MASE**	**ACF1**
Training set	-0.05	45.23	28.02	0.86	0.001

The ARIMA(5,0,0)(2,1,0)[12] is used to forecast the future values of the rainfall within Fada N'Gourma. The table 7 shows the forecast for the next 10 years.

Table 7 10-Year forecasting for Fada N'Gourma rainfall

Year	Pr(mm)	Year	Pr(mm)
2021	676.604078	2026	683.895678
2022	718.384769	2027	686.672948
2023	670.202231	2028	690.837555
2024	684.020538	2029	686.881626
2025	697.243504	2030	687.594675

Table 8 provides the results of the Mann-kendall and Sens'slope test. With a Z value of 0.89, the Mann Kendall test results show an increasing trend of rainfall over Fada N'Gourma up to 2030. The magnitude of the decrease is indicated by the sens' slope value, which is 0.88. Both trend statistic confirm a silght increase of rainfall within Fada N'Gourma by 2030.

Table 8 Values of the Sen's slope et Mann Kendall estimator for forecasted rainfall within Fada N'Gourma.

Sen's slope		
z	p-value	Sen's slope
0.894	0.37	0.88
MANN KENDALL		
z	p-value	Kendall Tau
0.894	0.37	0.244

4. Conclusion

Monthly rainfall has been investigated for Fada N'Gourma based on ARIMA forecasting model. Data spanning over a period of 1981 – 2022 was used to develop and test the models. The stationarity of the dataset has been checked based on Augmented Dicky fuller test. The study reveals that the best ARIMA model for monthly rainfall in Fada N'Gourma is the ARIMA (5,0,0)(2,1,0)[12]. The results highlited significant values of the statistical indicators. Base on ARIMA forecasting, the next ten years will be characterized by a slight upwarding trend of rainfall within the study are. This study reveals that ARIMA model can be selected as an appropriate forecasting tool to significantly predict the rainfall within Fada N'Gourma. The results may help in decision making.

Compliance with ethical standards

Acknowledgments

The authors are thankful to the Meteorological Department of Burkina Faso for providing valuable data.

Disclosure of conflict of interest

There are no conflicts of interest to disclose**.**

Funding

There is no financial support for publication of this paper**.**

References

[1] Adger, W. N., Huq, S., Brown, K., Conway, D., & Hulme, M. (2003). Adaptation to climate change in the developing world. Progress in development studies, 3(3), 179-195.

[2] Yair, A., & Raz-Yassif, N. (2004). Hydrological processes in a small arid catchment: scale effects of rainfall and slope length. Geomorphology, 61(1-2), 155-169.

[3] Cristiano, E., ten Veldhuis, M. C., & Van De Giesen, N. (2017). Spatial and temporal variability of rainfall and their effects on hydrological response in urban areas–a review. Hydrology and Earth System Sciences, 21(7), 3859-3878

[4] Van Loon, A. F. (2015). Hydrological drought explained. Wiley Interdisciplinary Reviews: Water, 2(4), 359-392.

[5] Niemczynowicz, J.: The rainfall movement – A valuable complement to short-term rainfall data, J. Hydrol., 104, 311–326, 1988.

[6] Connolly-Boutin, L., & Smit, B. (2016). Climate change, food security, and livelihoods in sub-Saharan Africa. Regional Environmental Change, 16, 385-399.

[7] Koffi, C. K., Djoudi, H., & Gautier, D. (2017). Landscape diversity and associated coping strategies during food shortage periods: evidence from the Sudano-Sahelian region of Burkina Faso. Regional Environmental Change, 17, 1369-1380.

[8] Nouaceur, Z., & Murarescu, O. (2020). Rainfall variability and trend analysis of rainfall in West Africa (Senegal, Mauritania, Burkina Faso). Water, 12(6), 1754.

[9] Guug, S. S., Abdul-Ganiyu, S., & Kasei, R. A. (2020). Application of SWAT hydrological model for assessing water availability at the Sherigu catchment of Ghana and Southern Burkina Faso. HydroResearch, 3, 124-133.

[10] Yonaba, R., Belemtougri, A., Tazen, F., Mounirou, L. A., Koïta, M., Karambiri, H., & Yacouba, H. (2022). Assessing the accuracy of SM2RAIN (Soil Moisture to Rainfall) products in poorly gauged countries: the case of Burkina Faso in the West African Sahel (No. IAHS2022-263). Copernicus Meetings

[11] Ibrahim, B., Karambiri, H., Polcher, J., Yacouba, H., & Ribstein, P. (2014). Changes in rainfall regime over Burkina Faso under the climate change conditions simulated by 5 regional climate models. Climate Dynamics, 42, 1363-1381.

[12] Messager, C., Gallée, H., Brasseur, O. et al. Influence of observed and RCM-simulated precipitation on the water discharge over the Sirba basin, Burkina Faso/Niger. Clim Dyn 27, 199–214 (2006).

[13] Geetha, A., & Nasira, G. M. (2016). Time-series modelling and forecasting: Modelling of rainfall prediction using ARIMA model. International Journal of Society Systems Science, 8(4), 361-372.

[14] Petropoulos, F., Apiletti, D., Assimakopoulos, V., Babai, M. Z., Barrow, D. K., Taieb, S. B.,& Ziel, F. (2022). Forecasting: theory and practice. International Journal of Forecasting, 38(3), 705-871.

[15] Everingham, Y. L., Clarke, A. J., & Van Gorder, S. (2008). Long lead rainfall forecasts for the Australian sugar industry. International Journal of Climatology: A Journal of the Royal Meteorological Society, 28(1), 111-117.

[16] Moeletsi, M. E., Mellaart, E. A. R., Mpandeli, N. S., & Hamandawana, H. (2013). The use of rainfall forecasts as a decision guide for small-scale farming in Limpopo Province, South Africa. The Journal of Agricultural Education and Extension, 19(2), 133-145

[17] Nhita, F. (2013, March). A rainfall forecasting using fuzzy system based on genetic algorithm. In 2013 International Conference of Information and Communication Technology (ICoICT) (pp. 111-115). IEEE.

[18] Guido, Z., Zimmer, A., Lopus, S., Hannah, C., Gower, D., Waldman, K., & Evans, T. (2020). Farmer forecasts: Impacts of seasonal rainfall expectations on agricultural decision-making in Sub-Saharan Africa. Climate Risk Management, 30, 100247

[19] Mukheibir, P. (2008). Water resources management strategies for adaptation to climate-induced impacts in South Africa. Water Resources Management, 22, 1259-1276

[20] Bai, Y., Bezak, N., Zeng, B., Li, C., Sapač, K., & Zhang, J. (2021). Daily runoff forecasting using a cascade long short-term memory model that considers different variables. Water Resources Management, 35, 1167-118.

[21] Shu, X., Peng, Y., Ding, W., Wang, Z., & Wu, J. (2022). Multi-step-ahead monthly streamflow forecasting using convolutional neural networks. Water Resources Management, 36(11), 3949-3964

[22] Raval, M., Sivashanmugam, P., Pham, V., Gohel, H., Kaushik, A., & Wan, Y. (2021). Automated predictive analytics tool for rainfall forecasting. Scientific Reports, 11(1), 17704

[23] Darji, M. P., Dabhi, V. K., & Prajapati, H. B. (2015, March). Rainfall forecasting using neural network: A survey. In 2015 international conference on advances in computer engineering and applications (pp. 706-713). IEEE

[24] Cheung, K., Yu, Z., Elsberry, R. L., Bell, M., Jiang, H., Lee, T. C., & Tsuboki, K. (2018). Recent advances in research and forecasting of tropical cyclone rainfall. Tropical Cyclone Research and Review, 7(2), 106-127

[25] French, M. N., Krajewski, W. F., & Cuykendall, R. R. (1992). Rainfall forecasting in space and time using a neural network. Journal of hydrology, 137(1-4), 1-31.

[26] Fahad, S., Su, F., Khan, S. U., Naeem, M. R., & Wei, K. (2023). Implementing a novel deep learning technique for rainfall forecasting via climatic variables: An approach via hierarchical clustering analysis. Science of The Total Environment, 854, 158760.

[27] Hossain, I., Rasel, H. M., Imteaz, M. A., & Mekanik, F. (2018). Long-term seasonal rainfall forecasting: efficiency of linear modelling technique. Environmental Earth Sciences, 77, 1-10.

[28] Kirshen, P. H., & Flitcroft, I. D. (2000, August). Use of seasonal precipitation forecasting to improve agricultural production in the Sudano-Sahel: an institutional analysis of Burkina Faso. In Natural resources forum (Vol. 24, No. 3, pp. 185-195). Oxford, UK: Blackwell Publishing Ltd.

[29] Roncoli, C., Kirshen, P., Ingram, K., & Jost, C. (2001). Burkina Faso-integrating indigenous and scientific rainfall forecasting.

[30] Ingram, K. T., Roncoli, M. C., & Kirshen, P. H. (2002). Opportunities and constraints for farmers of West Africa to use seasonal precipitation forecasts with Burkina Faso as a case study. Agricultural systems, 74(3), 331-349

[31] Mishra, A., Hansen, J. W., Dingkuhn, M., Baron, C., Traoré, S. B., Ndiaye, O., & Ward, M. N. (2008). Sorghum yield prediction from seasonal rainfall forecasts in Burkina Faso. Agricultural and forest meteorology, 148(11), 1798-1814.

[32] Mazzucato, V., & Niemeijer, D. (2000). Rethinking soil and water conservation in a changing society: A case study in eastern Burkina Faso. Wageningen University and Research.

[33] INSD) (2020), 5e Recensement Général de la Population et de l'Habitat (RGPH), 69 p.

[34] Box, G. (2013). Box and Jenkins: time series analysis, forecasting and control. In A Very British Affair: Six Britons and the Development of Time Series Analysis During the 20th Century (pp. 161-215). London: Palgrave Macmillan UK

[35] Yurekli K, Simsek H, Cemek B, Karaman S (2007) Simulating climatic variables by using stochastic approach. Build Environ 42:3493–3499

[36] Filder, T.N., Muraya, M.M. and Mutwiri, R.M., Application of Seasonal Autoregressive Moving Average Models to Analysis and Forecasting of Time Series Monthly Rainfall Patterns in Embu County, Kenya. Asian Journal of Probability and Statistics, pp.1-15, 2019

[37] Ariyo, A. A., Adewumi, A. O., & Ayo, C. K., Stock price prediction using the ARIMA model. In 2014 UKSim-AMSS 16th International Conference on Computer Modelling and Simulation pp. 106-112. (2014, March).

[38] Rayner, G. D., & MacGillivray, H. L. (2002). Numerical maximum likelihood estimation for the g-and-k and generalized g-and-h distributions. Statistics and Computing, 12(1), 57-75.

[39] Blume-Kohout, R. (2010). Hedged maximum likelihood quantum state estimation. Physical review letters, 105(20), 200504.

[40] Mazucheli, J., Menezes, A. F. B., & Nadarajah, S. (2017). mle. tools: An R Package for Maximum Likelihood Bias Correction. R J., 9(2), 268.

[41] Yue, S., & Pilon, P. (2004). A comparison of the power of the t test, Mann-Kendall and bootstrap tests for trend detection/Une comparaison de la puissance des tests t de Student, de Mann-Kendall et du bootstrap pour la détection de tendance. Hydrological Sciences Journal, 49(1), 21-37.

[42] Mondal, A., Kundu, S., & Mukhopadhyay, A. (2012). Rainfall trend analysis by Mann-Kendall test: A case study of north-eastern part of Cuttack district, Orissa. International Journal of Geology, Earth and Environmental Sciences, 2(1), 70-78.

[43] Şen, Z. (2017). Innovative trend significance test and applications. Theoretical and applied climatology, 127, 939-947.

[44] Montgomery, D.C., Jennings, C.L., Kulahci, M.: Introduction to time series analysis and forecasting. John Wiley & Sons (2015)

[45] Bandara, K., Hyndman, R. J., & Bergmeir, C. (2021). MSTL: A seasonal-trend decomposition algorithm for time series with multiple seasonal patterns. arXiv preprint arXiv:2107.13462.

[46] Dickey, D. A., & Fuller, W. A. (1981). Likelihood ratio statistics for autoregressive time series with a unit root. Econometrica: journal of the Econometric Society, 1057-1072